

Journal of Experimental Nanoscience

ISSN: (Print) (Online) Journal homepage: https://www.tandfonline.com/loi/tjen20

# Green synthesis of Iron oxide and Iron dioxide nanoparticles using *Euphorbia tirucalli*: characterization and antiproliferative evaluation against three breast cancer cell lines

**Ipeleng Kopano Rosinah Kgosiemang, Ayodeji Mathias Adegoke, Samson Sitheni Mashele & Mamello Patience Sekhoacha**

**To cite this article:** Ipeleng Kopano Rosinah Kgosiemang, Ayodeji Mathias Adegoke, Samson Sitheni Mashele & Mamello Patience Sekhoacha (2023) Green synthesis of Iron oxide and Iron dioxide nanoparticles using *Euphorbia tirucalli*: characterization and antiproliferative evaluation against three breast cancer cell lines, Journal of Experimental Nanoscience, 18:1, 2276276, DOI: 10.1080/17458080.2023.2276276

**To link to this article:** https://doi.org/10.1080/17458080.2023.2276276

© 2023 The Author(s). Published by Informa UK Limited, trading as Taylor & Francis Group.

View supplementary material

Published online: 07 Nov 2023.

Submit your article to this journal

View related articles

View Crossmark data

Full Terms & Conditions of access and use can be found at
https://www.tandfonline.com/action/journalInformation?journalCode=tjen20

JOURNAL OF EXPERIMENTAL NANOSCIENCE
2023, VOL. 18, NO. 1, 2276276
https://doi.org/10.1080/17458080.2023.2276276

Taylor & Francis
Taylor & Francis Group

OPEN ACCESS Check for updates

# Green synthesis of Iron oxide and Iron dioxide nanoparticles using *Euphorbia tirucalli*: characterization and antiproliferative evaluation against three breast cancer cell lines

Ipeleng Kopano Rosinah Kgosiemang[a], Ayodeji Mathias Adegoke[b,c], Samson Sitheni Mashele[a] and Mamello Patience Sekhoacha[b]

[a]Unit for Drug Discovery Research, Department of Health Sciences, Faculty of Health and Environmental Sciences, Central University of Technology, Bloemfontein, South Africa; [b]Department of Pharmacology, Faculty of Health Sciences, University of the Free State, Bloemfontein, South Africa; [c]Cancer Research and Molecular Biology Laboratories, Department of Biochemistry, College of Medicine, University of Ibadan, Ibadan, Nigeria

**ABSTRACT**

Researchers have become increasingly interested in nanoparticles made from plants because of their stability and large surface area. In the current study, iron oxide and iron dioxide nanoparticles were synthesized using aerial parts of the E. tirucalli as a reducing agent. The nanoparticles were analyzed using various techniques, including Ultraviolet-visible spectroscopy, Fourier Transform Infrared spectroscopy, X-ray diffractometer, X-ray photoelectron spectroscopy, X-ray energy dispersive spectroscopy, Scanning electron Microscopy, and Transmission Electron Microscopy. The nanoparticles were then investigated for their antiproliferative effect against MCF-7, SK-BR-3, MDA-MB231, and Vero cell lines. The results confirmed the formation of FeO and FeO2 nanoparticles by color change and a UV absorbance peak between 220–390 nm. EDS analysis showed traces of Fe and O, while TEM confirmed the nanoparticle size of 100 nm. FTIR showed a peak at 514 nm. The FeO-RT NPs demonstrated over 80% antiproliferative activity against the MCF-7 cell line at a concentration of 10 µg/mL. while doxorubicin, FeO-RT NPs, and DCM extract showed similar activity against the MDA-MB231 cell line at 10 and 1 g/mL concentrations. However, Vero and SK-BR-3 cell lines showed decreased antiproliferative activity. This study highlights the environmentally friendly use and safe application of iron oxide NPs in cancer therapy.

**ARTICLE HISTORY**
Received 28 August 2023
Accepted 23 October 2023

**KEYWORDS**
*Euphorbia tirucalli*; iron oxide NPs; iron dioxide NPs; antiproliferation; breast cancer cells

## 1. Introduction

Cancer is a significant public health concern worldwide, ranking second only to cardiovascular disease as a leading cause of death [1]. Breast cancer is now the most commonly

**CONTACT** Mamello Sekhoacha SekhoachaMP@ufs.ac.za Department of Pharmacology, Faculty of Health Sciences, University of the Free State (UFS), Bloemfontein, Free State, South Africa.
Supplemental data for this article can be accessed online at https://doi.org/10.1080/17458080.2023.2276276.
© 2023 The Author(s). Published by Informa UK Limited, trading as Taylor & Francis Group.
This is an Open Access article distributed under the terms of the Creative Commons Attribution-NonCommercial License (http://creativecommons.org/licenses/by-nc/4.0/), which permits unrestricted non-commercial use, distribution, and reproduction in any medium, provided the original work is properly cited. The terms on which this article has been published allow the posting of the Accepted Manuscript in a repository by the author(s) or with their consent.

diagnosed cancer worldwide, with 2.3 million new cases estimated in 2020, accounting for 11.7% of all cancer cases [2]. Unfortunately, 684,996 people died from the disease [2]. The COVID-19 pandemic regulations resulted in a rise in cancer mortality and morbidity rates due to delayed diagnosis and treatment, ultimately impacting global health and the economy negatively [3].

Breast cancer is not a single disease, but rather a group of diseases with different characteristics and clinical features. Because of this, there is no single treatment approach that can be effective for all types of breast cancer [3,4]. For example, positive receptor cancer cell lines such as MCF-7, BT474, KLP-4, SK-BR-3, and others can be treated with surgery, hormonal therapy, and chemotherapy, respectively [5]. However, triple-negative breast cancers such as MDA-MB231, BT-459, SUM185PE, and others are difficult to treat because they lack all three receptors [6]. Moreover, it is important to note that the current treatments have adverse side effects, are not selective, and have poor pharmacokinetics [7–9]. Therefore, to overcome these limitations, a new therapeutic approach concerning cancer treatment is urgently needed.

Nanoparticles (NPs) have caught the attention of many researchers in the field of diagnosis and treatment due to their versatile and beneficial characteristics. They have already been utilized for various purposes such as tumor imaging *in vivo*, bio-molecular profiling of cancer biomarkers, and targeted drug delivery [10]. The use of green chemistry to synthesize NPs is an eco-friendly, economical, and sustainable solution that has gained attention for its potential to reduce the use of hazardous chemicals and solvents, resulting in lower toxicity and fewer harmful by-products [11–14]. This approach also utilizes readily available natural resources, such as plant extracts or microorganisms, which reduces the need for expensive reagents and energy-intensive processes [15]. The versatility of this method enables the production of a wide range of NPs with varying properties, including size, shape, and surface chemistry, making it customizable for specific applications [16]. Furthermore, it generates lower waste by products, leading to reduced pollution [15]. It is also easily scalable, making it ideal for industrial applications that require large quantities of NPs [17]. This method utilizes natural and renewable resources such as bacteria, algae, fungi, and plant extracts as substitutes for traditional physical and chemical methods to convert precursor metal salts into metal NPs [18]. When using biological agents like plant extracts or enzymes for green synthesis, the NPs often retain some of the bioactive properties of the source material, which can be beneficial in applications like drug delivery and sensing [19]. Therefore, among all the natural sources available, plant extracts have received the most attention because they contain secondary metabolites that can effectively reduce and stabilize metal precursors during green synthesis [20]. *Euphorbia tirucalli*, belonging to the *Euphorbiaceae* family, originally comes from eastern tropical Africa but has spread to other parts of the continent, including South Africa [21]. This plant has shown various pharmacological activities, such as molluscicidal [22,23], antibacterial [24], antiherpetic [25], and anti-mutagenic properties [26]. The latex from the plant has also been found to have both co-carcinogenic [27] and anti-carcinogenic properties [28]. In the Northeast region of Brazil, locals use the latex of *E. tirucalli* for various medicinal purposes. It is believed to have antimicrobial and laxative properties, and can also be used to treat asthma, cough, earache, rheumatism, verrucae, cancer, chancre, epithelioma, sarcoma, and skin tumors. Additionally, it is sometimes used as a folk remedy against syphilis [25,29].

Metal oxide NPs are known for their unique physio-chemical and optoelectronic properties, making them highly important [30–32]. Among the various metal oxides, iron oxide NPs have garnered significant attention due to their low toxicity, superparamagnetic properties, surface area and volume ratio, protein immobilization, and potential use in

diagnostic magnetic resonance imaging (MRI), thermal therapy, and drug delivery [33]. In addition, they have demonstrated effectiveness in inhibiting MCF-7 cell lines in prior research [34]. However, no comparative study has been conducted to assess the antiproliferative effects of iron oxide and iron dioxide NPs against MCF-7, SK-BR-3, and MDA-MB231 cell lines.

Therefore, this study aimed to synthesize metal iron oxide and iron dioxide NPs using the aerial plant extract of *E. tirucalli* as a reducing agent, characterize the NPs, and compare their antiproliferative effect against three different subtypes of breast cancer cell lines. Our research focuses on investigating the potential anticancer properties of *E. tirucalli* against breast carcinoma.

## 2. Materials and Methods

### 2.1. Materials

In March 2017, the *E. tirucalli* plant species was commercially acquired from Gariep Nursery in Pretoria, South Africa (GPS coordinates 25°47′3″S, 28°18′58″E). Dr. Nolubabalo Matinise of iTHEMBA LABS, South Africa generously donated ferric nitrate nonahydrate salts. The extraction solvents, namely Hex, DCM, and methanol (MeOH), were purchased from Merck in South Africa. MCF-7, SK-BR-3, and MDA-MB231 cells were purchased from Cellonex in South Africa. Reagents including DMEM, trypan blue dye, and MTT salt were purchased from Sigma Aldrich in South Africa.

### 2.2. Methods

#### 2.2.1. Plant extraction and preparation

Upon arrival at the laboratory, the aerial parts of the plant were washed with tap water and chopped into smaller pieces. The pieces were then air-dried and ground into a fine powder.

#### 2.2.2. Preparation of FeO and $FeO_2$ nanoparticles

In order to synthesize NPs, the *E. tirucalli* finely ground powder weighing 30 g was boiled in distilled water at 80 °C for a duration of 2 h. Following this, the extract was divided into two beakers and mixed with 5 g of Ferric nitrate nonahydrate. These solutions were then placed on a magnetic stirrer, maintained at 60 °C for a period of 12 h, and closely observed for any changes in color which would indicate the formation of NPs. The resulting NP pellets were obtained by subjecting the solutions to centrifugation at 5000 rpm for 20 min, after which they were washed with double distilled water to remove any excess plant extract. These pellets were then dried in an oven at 80 °C for 2 h. Once dried, the NPs were annealed at 500 °C for a duration of 2 h to eliminate impurities and were subsequently stored at room temperature for characterization.

*2.2.3. Preparation of Euphorbia tirucalli aerial extracts for cell culture.* To extract compounds from the plant, a 10 g fine powder was sequentially extracted using various organic solvents (hexane, dichloromethane, methanol, and ethyl acetate) in 150 mL portions. The extraction process was carried out for 48 h on a shaker at room temperature. The resulting extracts were filtered and concentrated under reduced pressure at 45 °C using a rotary vacuum evaporator from Buchi labotech Switzerland. Finally, the extracts were dried under a fume hood and stored at 4 °C for future use.

#### 2.2.4. Characterization of synthesized nanoparticles

Characterization of FeO and $FeO_2$ NPs was conducted using the established protocol by Shunmugadevi and Palanisamyb [35], with slight modifications. UV spectroscopy was utilized to investigate the absorption patterns, employing the Multiskan Go 1.01.10 spectrophotometer. Fourier Transform Infrared Spectroscopy (FTIR) was used to identify the functional groups involved in the capping process, with the Thermo Nicolet Nexus 670 spectrometer measuring the spectrum. The structural properties of the NPs were examined using the Bruker D8 X-ray diffractometer. The NPs' chemical state was determined by using XPS with the Versa Probe XPS V1.4. The morphology and size of the particles were determined using SEM and TEM, respectively. The JEOL JEM 2010 UHR and Philips 100 transmission electron microscope were used for this purpose. Lastly, EDS was used to detect the nano constituents present in FeO and $FeO_2$ NPs. The Philips 100 transmission electron microscope was used for this process.

#### 2.2.5. Phytochemical screening

A phytochemical analysis was conducted on the aerial part of *E. tirucalli* using Yadav and Agarwala's [36] protocol, with some slight modification. Various tests were carried out to determine the presence or absence of alkaloids, glycosides, flavonoids, phenols, saponins, terpenoids, and tannins.

#### 2.2.6. Antiproliferation screening of Euphorbia extracts

*2.2.6.1. Cell culture.* The MCF-7, SK-BR-3, and MDA-MB231 cell lines were cultured using Dulbecco's modified eagle's medium (DMEM), DMEM: HAMS F12 (1:1), and Mc-Coy media, respectively. Each medium was supplemented with 10% fetal bovine serum (FBS) and the cells were kept in an environment with 37 °C temperature and 5% CO2 humidity in an incubator. When the cells reached 80% confluency, they were sub-cultured.

*2.2.6.2. Antiproliferative assay.* To facilitate easy harvesting, the cells were treated with Trypsin. An automated cell counter (Countess FI, life technology) was used to count the viable cells with trypan blue dye. 1 x $10^5$ cells/ml were then seeded into each well of a 96-well microtiter plate and incubated under the same conditions for 24 h. The cells were treated with unannealed and annealed NPs along with crude *E. tirucalli* at concentrations of 100, 10, and 1 µg/mL in triplicate for 48 h. Wells containing untreated cells were used as a negative control, while Doxorubicin drug was used as a positive control. Cell growth activity was measured using the tetrazolium dye (MTT assay) [37]. Cell viability and growth inhibition percentage were calculated, and graphs were plotted using Microsoft Excel 2008.

## 3. Results and discussion

### 3.1. Phytochemical analysis

In our previous research on *E. tirucalli*, we examined its phytochemicals and discovered the presence of tannins, glycosides, triterpenoids, and saponins [38]. These components are recognized for possessing anticancer and antioxidant properties, and also have the potential to reduce metal ions [39,40]. Additionally, plants that contain antioxidants typically have reducing abilities.

### 3.2. Synthesis of iron oxide and iron dioxide NPs

The aerial part of *E. tirucalli* was utilized as a reducing agent, leading to a noticeable shift in color from light brown to black upon the introduction of Ferric nitrate nonahydrate salt to the *E. tirucalli* extract, Figure 1. This indicates the stimulation of electrons and the formation of FeO and $FeO_2$ NPs. The formation of these NPs was caused by plant secondary metabolites specifically polyphenols that effectively reduced metal ions and stabilized the FeO NPs and $FeO_2$ NPs. These nanoparticles have phytochemicals attached to their surface that possess hydrophilic hydroxyl groups. These groups enable the nanoparticles to be evenly dispersed in aqueous solutions [41]. These results are consistent with those of katata-Seru et al. [42], who found a comparable color alteration from reddish brown to black, suggesting the presence of Fe NPs.

### 3.3. Characterization of synthesized NPs

#### 3.3.1. UV-vis spectrum of iron oxide and iron dioxide NPs

To analyze the formation of iron nanoparticles, a UV-vis spectrophotometer was utilized to measure the absorbance in the range of 200 – 1000 nm. The results, depicted in Figure 2a,b, exhibit two absorption peaks between 220 – 390 nm. Figure 1a displays peaks at 220 and 380 nm, whereas Figure 1b shows peaks at 230 and 390 nm. These absorption peaks are attributed to the formation of iron nanoparticles. The absorption peak at 220 nm are attributed to the presence of tannins and tritepenoids in *E. tirucalli* extract [41]. The 220 nm and 230 nm peaks are consistent with Pattanayak and Nayak's study [43], which suggests the presence of surface plasmon vibrations in metallic iron nanoparticle solutions. Furthermore, the peak observed at 390 nm is in line with the findings of Kumar and Prem's study [44], which identified the formation of iron oxide nanoparticles.

#### 3.3.2. FTIR spectrum analysis of iron oxide and iron dioxide NPs

FTIR spectroscopy was employed to investigate the functional groups within *E. tirucalli* and the synthesized iron NPs. The FTIR spectra of the iron NPs are shown on Figure 3a,b. The figures displayed peaks in the 500 – 4000 cm-1 range, specifically at 3350 cm-1, 1650 cm-1, 1150–1050 cm-1, 750 cm-1, and 514 cm-1. The 3350 cm-1 peak signifies the presence of O-H groups, potentially originating from phenols or water in the *E. tirucalli* plant [45]. At 1650 cm-1, the peak suggests hydrogen bonding between oxygen molecules in the iron oxide nanoparticles and hydrogen molecules in E. tirucalli, representing C = O




**Figure 1.** Green synthesis of $FeO/FeO_2$ NPs using aerial part of *E. tirucalli*.

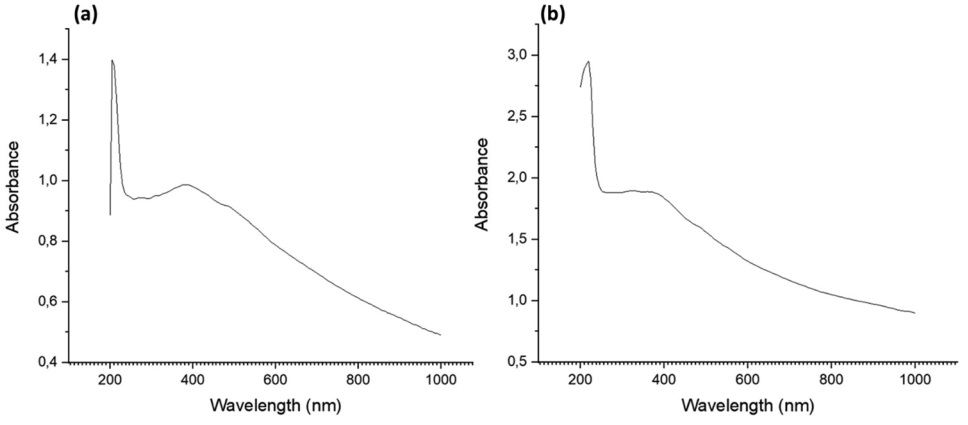



**Figure 2.** Ultraviolet visible spectroscopy of FeO (a) and $FeO_2$ (b) from *E. tirucalli*.

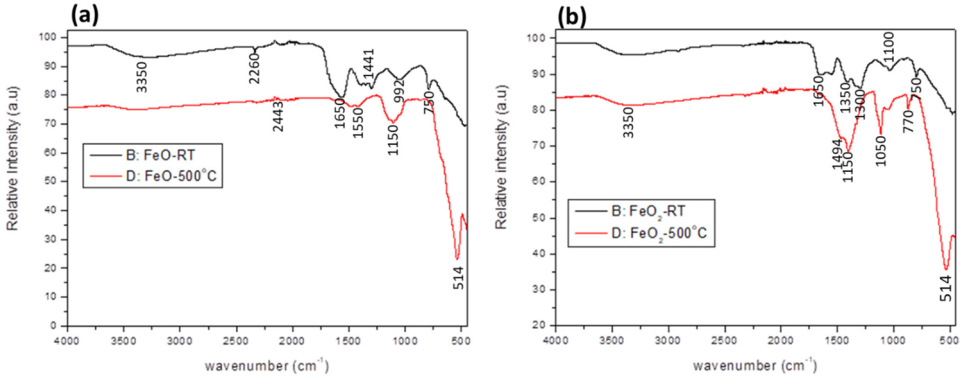



**Figure 3.** FTIR spectrum analysis of (a) iron oxide (FeO) and (b) iron dioxide ($FeO_2$) NPs reduced using *E. tirucalli*. Black line (B:FeO-RT) represents NPs at room temperature and red (D:$FeO_2$-500 °C)represent the annealed NPs at 500 °C.

stretching vibrations of amide-I [46,47]. The absorption peaks at 1150–1050 cm-1 are attributed to C-O groups, aligning with previous research confirming the formation of iron oxide nanoparticles [48]. The 750 cm-1 peak is due to CH groups present in aromatic compounds within *E. tirucalli*. Furthermore, the presence of a peak at 514 cm-1 confirms the formation of both iron oxide and dioxide nanoparticles, corroborating findings from earlier studies [34,47,49].

### *3.3.3. XRD analysis of iron oxide and iron dioxide NPs*

The XRD spectra of iron oxide and dioxide NPs synthesized using a green method are displayed in Figure 4a,b. The spectra showed various diffraction peaks at $2\theta = 30.91°$, 35.70°, 43.14°, 57.46°, and 62.90°, which correspond to the planer reflections of (220), (311), (222), (400), (511), and (440) of a cubic phase for both types of NPs, respectively. These peaks are attributed to (00-graphitic) [50]. These reflection peaks can be indexed to the magnetite structure of iron oxide observed in previous studies by Kumar and Prem [44], Perumal et al. [50], and Taha et al. [51], and can further be compared with the data found in JCPDS card (77–1545). However, additional peaks were detected in both samples, indicating the presence of impurities.

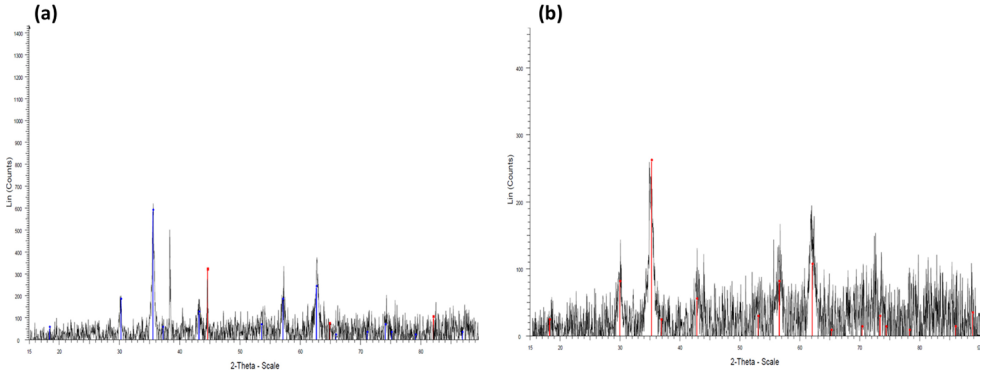



**Figure 4.** X-ray diffraction analysis of reduced FeO (a) and $FeO_2$ (b) NPs from *E. tirucalli* aerial parts after annealing.

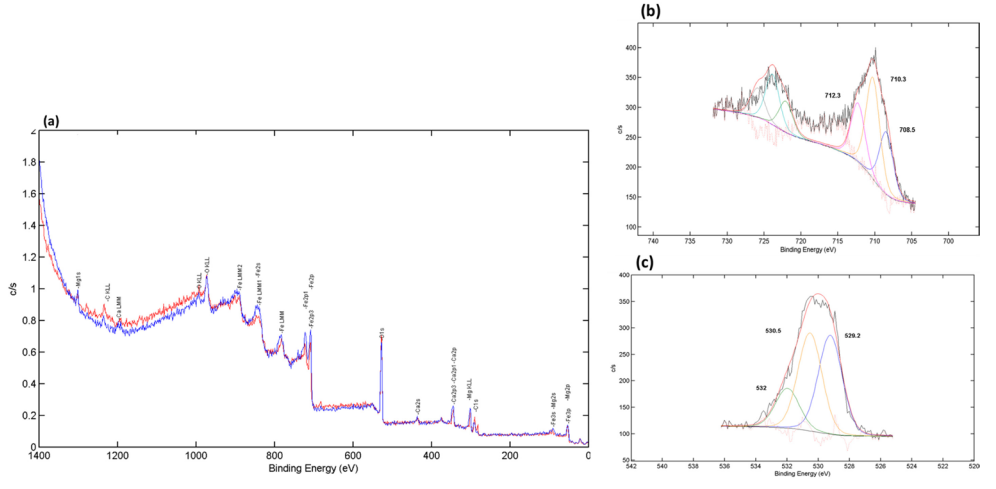



**Figure 5.** XPS analysis of $FeO_2$ NPs: high resolution $FeO_2$ scan (a); $FeO_2$-2p1 scan (b), $FeO_2$-O1s scan (c).

### *3.3.4. XPS analysis of iron dioxide NPs*

The XPS technique was employed to analyze the elemental composition and electron surface state of various components in $FeO_2$ NPs. Unfortunately, the analysis for FeO NP could not be completed as there was not enough material available. The resulting analysis, as shown in Figure 5a–c, revealed the presence of iron (Fe), magnesium (Mg), oxygen (O), carbon (C), and calcium (Ca) in $FeO_2$ NPs, thereby providing valuable insights into the chemical composition of the material. These findings were further affirmed through EDS analysis, which corroborated the presence of these elements in $FeO_2$ NPs. The peaks observed at 712.3, 710.3, and 708.5 eV were attributed to Fe 2p1, Fe 2p, and Fe p3, respectively, thereby providing evidence for the presence of Fe3+ octahedral species in the NP. These findings are consistent with previous studies [52] and highlight the importance of Fe3+ in the electronic properties of $FeO_2$ NPs. Moreover, the peaks observed at 530.5 eV and 532 eV were attributed to O 1s in the NPs and the presence of hydroxyl groups [53,54], respectively. Additionally, the peak observed at 529.2 eV indicated the presence of O on the surface of *E. tirucalli* $FeO_2$ NP, associated with O–H, O–C, and O = C compounds [55]. These findings suggest that the electronic properties of $FeO_2$ NPs are heavily influenced by the presence of O on the surface of the plant. Overall, the

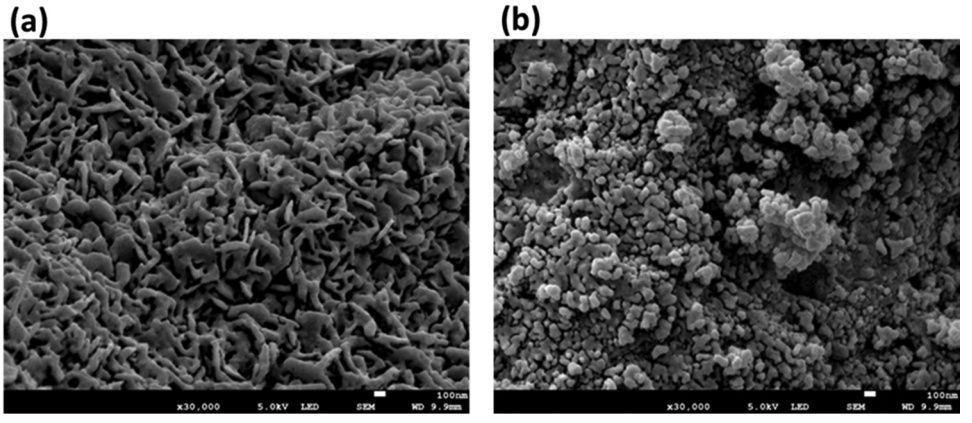



**Figure 6.** SEM imaging of (a) FeO and (b) $FeO_2$ observed at 100 nm.

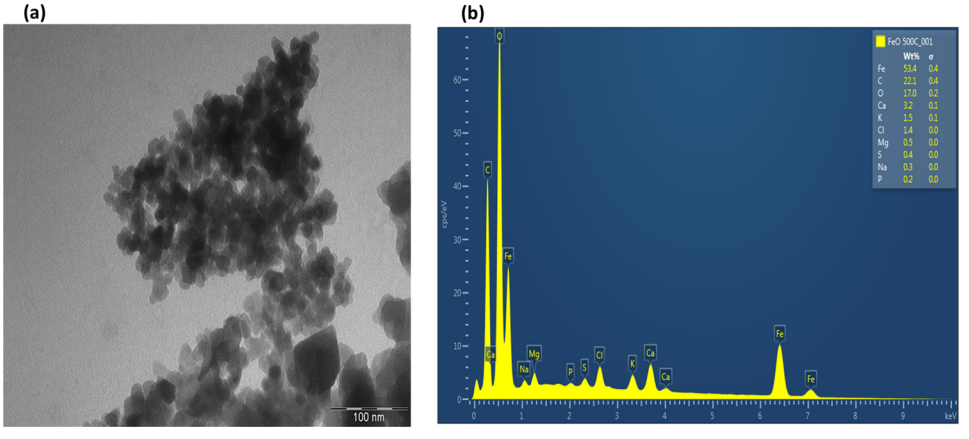



**Figure 7.** TEM imaging (a) and EDS analysis of FeO NPs synthesized using aerial parts of *E. tirucalli* (b).

valence states of Fe and O in $FeO_2$ NPs were found to be +3 and −2, respectively, as observed in the attributes of Fe 2p and O 1s core levels. These results provide valuable insights into the electronic properties of $FeO_2$ NPs and highlight the importance of understanding the elemental composition and electron surface state of materials in the field of nanotechnology.

### *3.3.5. SEM analysis of iron oxide and iron dioxide NPs*

The morphology and size of iron oxide and dioxide NPs were examined using a SEM. The nanoparticles were found to measure 100 nm in size, as illustrated in Figure 6a,b. Figure 6a depicts the iron oxide nanoparticles in a mesoporous and matrix-like arrangement, with a flat plate shape that can bend into a rod shape. In contrast, Figure 6b shows a different morphology compared to the iron oxide nanoparticles. Iron dioxide nanoparticles are formed in a spherical shape with a few cubic shapes and a clustered pattern. They may have clumped together due to the consistency of the solution and the drying method used [56]. The variation in morphology between the two iron nanoparticles could be attributed to the reducing power of phytochemicals, pH levels, or other factors that can affect their formation [57].

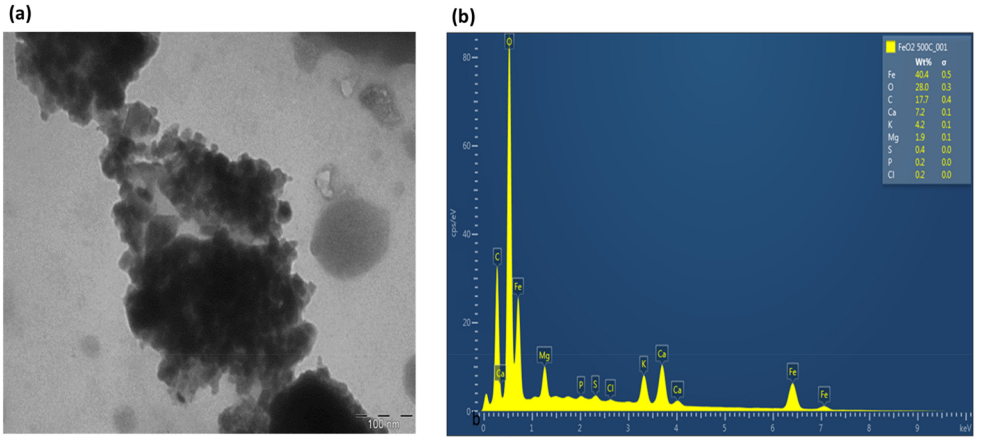



**Figure 8.** TEM imaging (a) and EDS analysis of $FeO_2$ NPs synthesized using aerial parts of *E. tirucalli* (b).

### *3.3.6. TEM and EDS analysis*

The TEM images in Figures 7a and 8a showcase the iron NPs that were synthesized, revealing hexagonal agglomerated NPs with a size of 100 nm. EDS profiling of all nanocomposites obtained after calcination indicated peaks, with a high characteristic peak of oxygen followed by carbon, iron, calcium, chloride, magnesium, potassium, sodium, sulphur and phosphorus present for both NPs in Figures 7b and 8b. Notably, sodium was not detected in the iron dioxide NP (Figure 8b). The presence of iron and oxygen confirmed the formation of iron oxide and dioxide NPs. The high oxygen and carbon peaks detected in both NPs suggest that polyphenols were involved in the synthesis of iron nanoparticles [58]. Furthermore, the oxygen and carbon peaks may represent the polyphenol present in the plant [59]. Additional weak composite peaks observed of calcium, sodium, and magnesium may arise from the glass that holds the sample during synthesis [52]. The phosphorus, potassium, sulphur, and chloride peaks observed were due to improper washing of the sample [60].

The composition of the iron oxide NPs was 53.4% of iron, 22.1% of carbon, 17.0% of oxygen, and all other composites were less than 5% (Figure 7b). On the other hand, the iron dioxide NPs were composed of 40.4% of iron, 28.0% of oxygen, 17.7% of carbon, 7.2% of calcium, and all other composites were less than 5% (Figure 8b). The difference in oxygen percentages between the iron oxide and iron dioxide NPs can be attributed to their formation process. They are both formed from Ferric nitrate nonahydrate precursor salt when iron reacts with oxygen from the plant extract's metabolic constituents. Sometimes, when the oxygen from the water or air binds to iron, it increases the number of oxygen molecules within the compound, differentiating between the two oxides. The presence of oxygen and carbon is crucial as they stabilize and reduce the two metal oxides [61]. Although there were impurities present in the samples, they were in low concentrations, as shown in the results.

### *3.3.7. MTT assay*

Breast cancer is characterized by the protein expression of estrogen receptor (ER), progesterone receptor (PR), and human epidermal growth factor receptor 2 (HER2). Because of these characteristics, it is necessary to compare the effects of the potential antiproliferation drugs or drug carriers in different breast cancer cells with clinically approved cancer drugs in order to assess the efficacy or potential benefits within new application techniques.

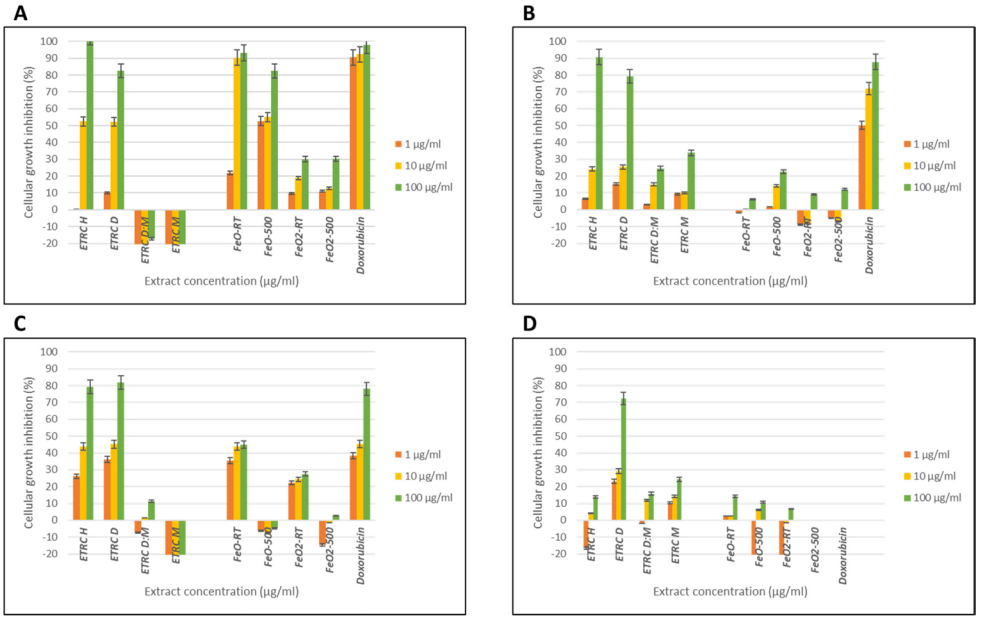



**Figure 9.** Cell growth inhibition % of four *Euphorbia* crude extracts, FeO-RT, FeO-500, $FeO_2$-RT and $FeO_2$-500 NPs against MCF-7 (a), SK-BR-3 (B), MDA-MB231 (C) and Vero (D). *E. tirucalli* hexane (*ETRC* Hex) extract, *E. tirucalli* Dichloromethane (*ETRC* DCM), *E. tirucalli* Dichloromethane: Methanol (*ETRC* DCM: MeOH), *E. tirucalli* methanol (*ETRC* MeOH), iron oxide unannealed NPs (FeO-RT), iron oxide annealed NPs (FeO-500), iron dioxide unannealed NPs ($FeO_2$-RT) and iron dioxide annealed NPs ($FeO_2$-500). Doxorubicin (standard drug).
*$FeO_2$-500 NPs was not tested on Vero cell line.

Antiproliferative effect of the crude extracts, annealed and unannealed Iron Oxide and Iron dioxide NPs against MCF-7, SKBR-3, MDA-MB231 and Vero cell lines was tested across concentrations of 1, 10, and 100 µg/mL in triplicates, and doxorubicin served as a standard drug. The level of toxicity exhibited by the treatment was observed to be concentration-dependent, with the most substantial toxicity observed at the highest concentration, Figure 9a–d.

The extracts from *E. tirucalli*, specifically Hex and DCM, displayed moderate antiproliferative effects against MCF-7 and MDA-MB231 cells. At concentrations of 100 and 10 µg/mL, these extracts inhibited cell growth by over 50% and 40%, respectively. However, the same extracts showed weak activity against SK-BR-3 and Vero cells, with cell growth inhibition rates of less than 40%. This suggests that SK-BR-3 is less susceptible to the extracts than MCF-7 and MDA-MB231. Previous research has also shown that stevioside and other compounds have higher cytotoxicity against MDA-MB231 and MCF-7 cell lines compared to SK-BR-3 cell line [62,63]. This anticancer activity could be due to estrogen and progesterone receptors as both cell lines are HER2 negative [62]. Additionally, $Fe_3O_4$NPs were reported to inhibit the growth of lung cancer cells Habibi et al. [64]. Moreover, Rajendran et al. [65] have demonstrated a considerable level of $Fe_2O_3$NPs cytotoxicity against various cancer cells, especially at lower concentrations, in comparison to normal cells. In a study conducted by Al-Shalabi et al. [66], it was found that IONPs were highly effective in inhibiting the growth of the MDA-MB231 cell line. The $IC_{50}$ value was measured at 0.3817 µg/mL, indicating a strong inhibitory effect. According to a research conducted by Pillai and colleagues [67], IONPs have been found to possess remarkable cytotoxicity against DLD-1 cancer cells. Interestingly, these nanoparticles have been

demonstrated to have minimal or no adverse effects on normal cells, thus making them a potentially efficient option for treating cancer. This finding suggests that IONPs may have potential as a therapeutic agent for breast cancer treatment.

Moreover, the synthesized unannealed FeO-RT NPs showed potent activity against MCF-7 cells with over 80% inhibitory activity at concentrations of 100 and 10 µg/mL, which could be attributed to impurities and compounds present in the plant before calcination. After calcination, the antiproliferative activity decreased, indicating the degradation of phytochemicals due to increased temperature. Additionally, the annealed and unannealed FeO NPs showed higher inhibitory activity against MCF-7 than the Hex and DCM extracts, and about the same as the standard drug. Contrary, studies by Hernandes et al. [68] reported a 20% decrease in cell viability when MCF-7 and HeLa cells were treated with mesoporous silica NPs. Moreover, other studies revealed that MCF-7 cells treated with pure/uncoated iron oxide NPs had high cell viability [69].

The FeO NPs and doxorubicin standard drug showed almost the same activity at 10 and 1 µg/mL concentrations against MDA-MB231, indicating moderate activity against the cell line. This activity shows the potential of FeO as a promising antiproliferative agent. The $FeO_2$ NPs showed decreased cell growth inhibition activity compared to the FeO NPs, which could be attributed to the chemicals and bonding abilities of $FeO_2$ and FeO.

## 4. Conclusion

Iron oxide and iron dioxide NPs were successfully synthesized using the aerial parts of *Euphorbia tirucalli*. The synthesized FeO-RT NPs together with the Hex and DCM extracts showed increased antiproliferative activity against MCF-7 and MDA-231 breast cancers compared to SK-BR-3 and Vero cells. The results show that the triple-negative breast cancer is not restricted to the receptor binding mode of action. The decreased antiproliferative activity against SK-BR-3 cells should be investigated further to determine the mechanism of action of the NPs and extracts. Further cytotoxic analysis should be conducted to determine the selectivity of the NPs and extracts. In conclusion, this study confirmed that the green-synthesized FeO NPs could be a potential antiproliferative drug because of the safety it displayed with the Vero cells.

## Disclosure statement

The authors declare no conflict of interest.

## Funding

This study was financially supported by the NRF [grant numbers 105946 and 108456], and the Innovation fund from the Central University of Technology, Free State.

## References

1. Kocarnik JM, Compton K, Dean FE, et al. Cancer incidence, mortality, years of life lost, years lived with disability, and Disability-Adjusted life years for 29 cancer groups from 2010 to 2019. JAMA Oncol. 2022;*8*(3):1. doi: 10.1001/jamaoncol.2021.6987.
2. Sung H, Ferlay J, Siegel RL, et al. Global cancer statistics 2020: GLOBOCAN estimates of incidence and mortality worldwide for 36 cancers in 185 countries. CA Cancer J Clin. 2021;*71*(3):209–14. doi: 10.3322/caac.21660.

3. Siegel RL, Miller KD, Fuchs HE, et al. Cancer statistics, 2021. CA Cancer J Clin. 2021;*71*(1):7–33. doi: 10.3322/caac.21654.
4. Polyak K. Breast cancer: origins and evolution. J Clin Invest. 2007;*117*(11):3155–3163. doi: 10.1172/jci33295.
5. Moo T-A, Sanford R, Dang C, et al. Overview of breast cancer therapy. PET Clin. 2018;*13*(3):339–354. doi: 10.1016/j.cpet.2018.02.006.
6. Zagami P, Carey LA. Triple negative breast cancer: pitfalls and progress. NPJ Breast Cancer. 2022;*8*(1):95. doi: 10.1038/s41523-022-00468-0.
7. Nurgali K, Rudd JA, Was H, et al. Editorial: cancer therapy: the challenge of handling a double-edged sword. Front Pharmacol. 2022;*13*:1007762. doi: 10.3389/fphar.2022.1007762.
8. Pucci C, Martinelli C, Ciofani G. Innovative approaches for cancer treatment: current perspectives and new challenges. Ecancermedicalscience. [online]2019;*13*(1):961. doi: 10.3332/ecancer.2019.961.
9. Zugazagoitia J, Guedes C, Ponce S, et al. Current challenges in cancer treatment. Clin Ther. 2016;*38*(7):1551–1566. doi: 10.1016/j.clinthera.2016.03.026.
10. Rocha M, Chaves N, Báo S. Nanobiotechnology for breast cancer treatment. Breast Cancer Biol Med. 2017:411–432. doi: 10.5772/66989.
11. Mittal AK, Chisti Y, Banerjee UC. Synthesis of metallic nanoparticles using plant extracts. Biotechnol Adv. 2013;*31*(2):346–356. doi: 10.1016/j.biotechadv.2013.01.003.
12. Iravani S. Green synthesis of metal nanoparticles using plants. Green Chem. 2011;*13*(10):2638. doi: 10.1039/c1gc15386b.
13. Chandran SP, Chaudhary M, Pasricha R, et al. Synthesis of gold nanotriangles and silver nanoparticles using aloe vera plant extract. Biotechnol Prog. 2006;*22*(2):577–583. doi: 10.1021/bp0501423.
14. Huang J, Li Q, Sun D, et al. Biosynthesis of silver and gold nanoparticles by novel sundriedCinnamomum camphoraleaf. Nanotechnology. 2007;*18*(10):105104. doi: 10.1088/0957-4484/18/10/105104.
15. Ahmed SF, Mofijur M, Rafa N, et al. Green approaches in synthesising nanomaterials for environmental nanobioremediation: technological advancements, applications, benefits and challenges. Environ Res. 2022;*204*(Pt A):111967. doi: 10.1016/j.envres.2021.111967.
16. Álvarez-Chimal R, Arenas-Alatorre J. Green synthesis of nanoparticles. A biological approach. IntechOpen eBooks. 2023;1–18. doi: 10.5772/intechopen.1002203.
17. Altammar KA. A review on nanoparticles: characteristics, synthesis, applications, and challenges. Front Microbiol. 2023;*14*:1155622. doi: 10.3389/fmicb.2023.1155622.
18. Pandit C, Roy A, Ghotekar S, et al. Biological agents for synthesis of nanoparticles and their applications. J King Saud Univ Sci. 2022;*34*(3):101869. doi: 10.1016/j.jksus.2022.101869.
19. Noah NM, Ndangili PM. Green synthesis of nanomaterials from sustainable materials for biosensors and drug delivery. Sens Int. 2022;*3*:100166. doi: 10.1016/j.sintl.2022.100166.
20. Jan H, Shah M, Andleeb A, et al. Plant-Based synthesis of zinc oxide nanoparticles (ZnO-NPs) using aqueous leaf extract of aquilegia pubiflora: their antiproliferative activity against HepG2 cells inducing reactive oxygen species and other *in vitro* properties. Oxid Med Cell Longev. 2021;*2021*: e4786227–14. doi: 10.1155/2021/4786227.
21. Ernst M, Grace OM, Saslis-Lagoudakis CH, et al. Global medicinal uses of *euphorbia* L.(*Euphorbiaceae*). J Ethnopharmacol. 2015;*176*:90–101. doi: 10.1016/j.jep.2015.10.025.
22. Jurberg P, Cabral Neto JB, Schall VT. Molluscicide activity of the 'avelós' plant (*Euphorbia tirucalli*, L.) on biomphalaria glabrata, the mollusc vector of schistosomiasis. Mem Inst Oswaldo Cruz. 1985;*80*(4):423–427. doi: 10.1590/s0074-02761985000400007.
23. Tiwari S, Singh P, Singh A. Toxicity of *euphorbia tirucalli* plant against freshwater target and non-target organisms. Pakistan J Biol Sci. 2003;*6*(16):1423–1429. doi: 10.3923/pjbs.2003.1423.1429.
24. Lirio LG, Hermano ML, Fontanilla MQ. Note antibacterial activity of medicinal plants from the Philippines. Pharm Biol. 1998;*36*(5):357–359. doi: 10.1076/phbi.36.5.357.4656.
25. Betancur-Galvis L, Morales G, Forero J, et al. Cytotoxic and antiviral activities of colombian medicinal plant extracts of the *euphorbia* genus. Mem Inst Oswaldo Cruz. 2002;*97*(4):541–546. doi: 10.1590/s0074-02762002000400017.
26. Ruiz Rezende J, Baroni Rodrigues S, Aparecida Soares Jabor I, et al. Antimutagenic effect of the *euphorbias* latex in Aspergillus nidulans methionine system. Acta Sci Biol Sci. 2004;*26*(4):481–484. doi: 10.4025/actascibiolsci.v26i4.1531.
27. Gschwendt M, Hecker E. Tumor-promoting compounds from *euphorbia* cooperi di- and triesters of 16-hydroxy-12-desoxy-phorbol. Tetrahedron Lett. 1970;*11*(8):567–570. doi: 10.1016/s0040-4039(01)97771-8.
28. Hecker E. Cocarcinogenic principles from the seed oil of croton tiglium and from other euphorbiaceae. Cancer Res. 1968;*28*(11):2338–2348.

29. Silva ACP, Faria D D, Borges NdE, et al. Toxicological screening of euphorbia tirucalli L.: developmental toxicity studies in rats. J Ethnopharmacol. 2007;*110*(1):154–159. doi: 10.1016/j.jep.2006.09.012.
30. Wang M, Thanou M. Targeting nanoparticles to cancer. Pharmacol Res. 2010;*62*(2):90–99. doi: 10.1016/j.phrs.2010.03.005.
31. Hao R, Xing R, Xu Z, et al. Synthesis, functionalization, and biomedical applications of multifunctional magnetic nanoparticles. Adv Mater. 2010;*22*(25):2729–2742. doi: 10.1002/adma.201000260.
32. Thema FT, Manikandan E, Gurib-Fakim A, et al. Single phase bunsenite NiO nanoparticles green synthesis by agathosma betulina natural extract. J Alloys Compd. 2016;*657*:655–661. doi: 10.1016/j.jallcom.2015.09.227.
33. Kulpa-Koterwa A, Ossowski T, Niedziałkowski P. Functionalized Fe3O4 nanoparticles as glassy carbon electrode modifiers for heavy metal ions detection—a mini review. Materials. 2021;*14*(24):7725. doi: 10.3390/ma14247725.
34. Sulaiman GM, Tawfeeq AT, Naji AS. Biosynthesis, characterization of magnetic iron oxide nanoparticles and evaluations of the cytotoxicity and DNA damage of human breast carcinoma cell lines. Artif Cells Nanomed Biotechnol. 2018;*46*(6):1215–1229. doi: 10.1080/21691401.2017.1366335.
35. Shunmugadevi C, Palanisamy P. Comparative Study of Silver Nanoparticles: Green Synthesis, Characterization and Biological Evaluation of Carica papaya and Andrographis paniculata Leaf Extract. [online] *Semantic Scholar*. 2016. Available from: https://www.semanticscholar.org/paper/Comparative-Study-of-Silver-Nanoparticles%3A-Green-of-Shunmugadevi Palanisamy/190cc92dad896af989591149ebcea4857cc3ca65
36. Yadav RNS, Agarwala M. Phytochemical analysis of some medicinal plants. J Phytol. 2011;3(12):10–14 .
37. Munro B, Vuong Q, Chalmers A, et al. Phytochemical, antioxidant and anti-Cancer properties of euphorbia tirucalli methanolic and aqueous extracts. Antioxidants (Basel). 2015;*4*(4):647–661. doi: 10.3390/antiox4040647.
38. Kgosiemang IK, Lefojane R, Direko P, et al. Green synthesis of magnesium and cobalt oxide nanoparticles using euphorbia tirucalli: characterization and potential application for breast cancer inhibition. Inorg Nano-Metal Chem. 2020;*50*(11):1070–1080. doi: 10.1080/24701556.2020.1735422.
39. Laszczyk MN. Pentacyclic triterpenes of the lupane, oleanane and ursane group as tools in cancer therapy. Planta Med. 2009;*75*(15):1549–1560. doi: 10.1055/s-0029-1186102.
40. Almehdar H, Abdallah HM, Osman A-MM, et al. In vitro cytotoxic screening of selected saudi medicinal plants. J Nat Med. 2012;*66*(2):406–412. doi: 10.1007/s11418-011-0589-8.
41. Kiwumulo HF, Muwonge H, Ibingira C, et al. Green synthesis and characterization of iron-oxide nanoparticles using moringa oleifera: a potential protocol for use in low and Middle income countries. BMC Res Notes. 2022;*15*(1):149. doi: 10.1186/s13104-022-06039-7.
42. Katata-Seru L, Moremedi T, Aremu OS, et al. Green synthesis of iron nanoparticles using moringa oleifera extracts and their applications: removal of nitrate from water and antibacterial activity against Escherichia coli. J Mol Liq. 2018;*256*:296–304. doi: 10.1016/j.molliq.2017.11.093.
43. Pattanayak M, Nayak PL. Green synthesis and characterization of zero valent iron nanoparticles from the leaf extract of azadirachta indica (neem). World J Nano Sci Technol. 2013;*2*(1):06–09. doi: 10.5829/idosi.wjnst.2013.2.1.21132.
44. Viju Kumar VG, Prem A. Green synthesis and characterization of iron oxide nanoparticles using phyllanthus niruri extract. Orient J Chem. 2018;*34*(5):2583–2589. doi: 10.13005/ojc/340547.
45. Elumalai K, Velmurugan S. Green synthesis, characterization and antimicrobial activities of zinc oxide nanoparticles from the leaf extract of azadirachta indica (L.). Appl Surf Sci. 2015;*345*:329–336. doi: 10.1016/j.apsusc.2015.03.176.
46. Jubb AM, Eskelsen JR, Yin X, et al. Characterization of iron oxide nanoparticle films at the air–water interface in arctic tundra waters. Sci Total Environ. 2018;*633*:1460–1468. doi: 10.1016/j.scitotenv.2018.03.332.
47. Pal S. *Antimicrobial activity of iron oxide nanoparticles*. [online] ethesis.nitrkl.ac.in. National Institute of Technology, India [Doctoral dissertation]. 2014. Available from: http://ethesis.nitrkl.ac.in/5598/.
48. Wang B, Blin T, Käkinen A, et al. Brushed polyethylene glycol and phosphorylcholine for grafting nanoparticles against protein binding. Polym Chem. 2016;*7*(45):6875–6879. doi: 10.1039/c6py01480a.
49. Kumar Das A, Marwal A, Verma R. Bio-Reductive synthesis and characterization of plant protein coated magnetite nanoparticles. NH. 2014;*7*:69–86. doi: 10.4028/www.scientific.net/NH.7.69.
50. Perumal S, Atchudan R, Lee YR. Synthesis of Water-Dispersed sulfobetaine methacrylate–iron oxide Nanoparticle-Coated graphene composite by free radical polymerization. Polymers (Basel). 2022;*14*(18):3885. doi: 10.3390/polym14183885.

51. Taha AB, Essa MS, Chiad BT. Spectroscopic study of iron oxide nanoparticles synthesized via hydrothermal method. Chem. Methodol. 2022;*6*(12):977–984. doi: 10.22034/chemm.2022.355199.1590.
52. Sridevi H, Bhat MR, Kumar PS, et al. Structural characterization of cuboidal α-Fe2O3 nanoparticles synthesized by a facile approach. Appl Nanosci. 2023;*13*(8):5605–5613. doi: 10.1007/s13204-023-02780-y.
53. Miri A, Najafzadeh H, Darroudi M, et al. Iron oxide nanoparticles: biosynthesis, magnetic behavior, cytotoxic effect. ChemistryOpen. 2021;*10*(3):327–333. doi: 10.1002/open.202000186.
54. Ba-Abbad MM, Benamour A, Ewis D, et al. Synthesis of Fe3O4 nanoparticles with different shapes through a Co-Precipitation method and their application. JOM. 2022;*74*(9):3531–3539. doi: 10.1007/s11837-022-05380-3.
55. Justus J, Roy SDD, Saravanakumar K, et al. Judging phase purity of hematite ($\alpha$-$Fe_2O_3$) nanoparticles through structural and magnetic studies. Mater Res Express. 2021;*8*(5):055005–055005. doi: 10.1088/2053-1591/abff09.
56. Rahman SSU, Qureshi MT, Sultana K, et al. Single step growth of iron oxide nanoparticles and their use as glucose biosensor. Results Phys. 2017;*7*:4451–4456. doi: 10.1016/j.rinp.2017.11.001.
57. Truskewycz A, Shukla R, Ball AS. Phytofabrication of iron nanoparticles for hexavalent chromium remediation. ACS Omega. 2018;*3*(9):10781–10790. doi: 10.1021/acsomega.8b00410.
58. Clarina T, Flomina PJ, Thangeswari P, et al. Polpala flower extract mediated one step green synthesis and characterization of magnetite (Fe3O4) nanoparticles. Asia Jour Rese Chem. 2018;*11*(2):459–462. doi: 10.5958/0974-4150.2018.00083.4.
59. Ahmed HM, El-Khateeb MA, Sobhy NA, et al. Green synthesis of magnetite nanoparticles using waste natural materials and its application for wastewater treatment. Environ Sci Proc. 2023;*25*(1):99. doi: 10.3390/ecws-7-14181.
60. Yadav VK, Ali D, Khan SH, et al. Synthesis and characterization of amorphous iron oxide nanoparticles by the sonochemical method and their application for the remediation of heavy metals from wastewater. Nanomaterials (Basel). 2020;*10*(8):1551. doi: 10.3390/nano10081551.
61. Afsheen S, Tahir MB, Iqbal T, et al. Green synthesis and characterization of novel iron particles by using different extracts. J Alloys Compd. 2018;*732*:935–944. doi: 10.1016/j.jallcom.2017.10.137.
62. Parvathaneni V, Chilamakuri R, Kulkarni NS, et al. Exploring amodiaquine's repurposing potential in breast cancer treatment—assessment of in-Vitro efficacy & mechanism of action. Int J Mol Sci. 2022;*23*(19):11455. doi: 10.3390/ijms231911455.
63. Khare N, Chandra S. Stevioside mediated chemosensitization studies and cytotoxicity assay on breast cancer cell lines MDA-MB-231 and SKBR3. Saudi J Biol Sci. 2019;*26*(7):1596–1601. doi: 10.1016/j.sjbs.2018.10.009.
64. Habibi A, Sadat A, Salehzadeh A, et al. Novel pyridinecarboxaldehyde thiosemicarbazone conjugated magnetite nanoparticulates (MNPs) promote apoptosis in human lung cancer A549 cells. J Biol Inorg Chem. 2020;*25*(1):13–22. doi: 10.1007/s00775-019-01728-4.
65. Rajendran K, Sen S, G S, et al. Evaluation of cytotoxicity of hematite nanoparticles in bacteria and human cell lines. Colloids Surf B Biointerfaces. 2017;*157*:101–109. doi: 10.1016/j.colsurfb.2017.05.052.
66. Al-Shalabi R, Abu-Huwaij R, Hamed R, et al. The antimicrobial and the antiproliferative effect of human triple negative breast cancer cells using the greenly synthesized iron oxide nanoparticles. J Drug Delivery Sci Technol. 2022;*75*:103642–103642. doi: 10.1016/j.jddst.2022.103642.
67. Pillai RR, Sreelekshmi PB, Meera AP, et al. Biosynthesized iron oxide nanoparticles: cytotoxic evaluation against human colorectal cancer cell lines. Mater Today: proc. 2022;*50*:187–195. doi: 10.1016/j.matpr.2022.01.151.
68. Hernandes EP, Bini RD, Endo KM, et al. Doxorubicin-Loaded magnetic nanoparticles: enhancement of doxorubicin's effect on breast cancer cells (MCF-7). Magnetochemistry. 2022;*8*(10):114. doi: 10.3390/magnetochemistry8100114.
69. Ghosh S, More P, Derle A, et al. Diosgenin functionalized iron oxide nanoparticles as novel nanomaterial against breast cancer. J Nanosci Nanotechnol. 2015;*15*(12):9464–9472. doi: 10.1166/jnn.2015.11704.